The Contribution of Perfusion MR and MR Spectroscopy Sequences to Conventional Sequences in the Staging of Glial Tumors

Perfüzyon MR ve MR Spektroskopi Sekanslarının Glial Tümörlerin Evrelendirilmesinde Konvansiyonel Sekanslara Katkısı

Suat Kubat[1] Türkan İkizceli[2]

[1]Erciyes University, Faculty of Medicine, Department of Radiology, Kayseri, Turkey
[2]University of Health Sciences, Haseki Training and research Hospital, Department of Radiology, Istanbul, Turkey

ABSTRACT

Aim: To demonstrate their contribution to staging by adding Perfusion Magnetic Resonance Imaging (MRP) and Magnetic Resonance Spectroscopy (MRS) to conventional Magnetic Resonance Imaging (MRI) sequences in cerebral glial tumor cases.
Material and Methods: Twenty-six patients (F/M:12/14, mean age 45.6±17.3) with primary glial tumors on MRI were included in the study prospectively. The lesions included in the study were single lesions, supratentorial and inter-axial localization. All lesions were diagnosed histopathologically. Conventional MRI, MRP and MRS images were taken sequentially in a single session to all patients. The parameters obtained from these images were analyzed statistically.
Results: For low/high stage tumor differentiation, the sensitivity of conventional MRI staging was 100% with a specificity of 57%. Separately assessing the sensitivity and specificity rates for conventional MRI, MRP and MRS, the combined use of conventional MRI+MRP (rCBV), conventional MRI+MRS (Lipid Lactate [LL] peak) and conventional MRI+MRP (rCBV)+MRS (LL peak) were observed to increase the specificity rates of conventional MRI. Relative cerebral blood volume (rCBV) value and LL peak was found to be significant for the differentiation of low-stage/high-stage brain tumors.
Conclusion: The conventional MRI has high sensitivity and low specificity for preoperative glioma staging. The specificity of conventional MRI findings increases when MRP and MRS are added to it.

Keywords: *Glial cell tumors, perfusion magnetic resonance imaging, magnetic resonance spectroscopy*

ÖZ

Amaç: Serebral glial tümör olgularında konvansiyonel Manyetik Rezonans Görüntüleme (MRG) sekanslarına Perfüzyon MR (MRP) ve MR Spektroskopi (MRS) eklenerek evrelemeye katkılarını göstermek.
Gereç ve Yöntemler: MRG'de primer gliyal tümörlü 26 hasta (K/A: 12/14, ortalama yaş 45.6±17.3) prospektif olarak çalışmaya alındı. Çalışmaya dahil edilen lezyonlar tek lezyonlar, supratentoryal ve intra-aksiyel lokalizasyon idi. Tüm lezyonlara histopatolojik olarak tanı konuldu. Tüm hastalara tek bir seansta konvansiyonel MRG, MRP ve MRS görüntüleri alındı. Bu görüntülerden elde edilen parametreler istatistiksel olarak analiz edildi.
Bulgular: Düşük/yüksek evre tümör evrelemesi için konvansiyonel MRG evrelemesinin duyarlılığı %100 ve özgüllük ise %57 idi. Konvansiyonel MRG, MRP ve MRS için duyarlılık ve özgüllük oranlarının ayrı ayrı değerlendirilmesi, konvansiyonel MRG+MRP (rCBV), konvansiyonel MRG+MRS (lipit laktat [LL] piki) ve konvansiyonel MRG+MRP (rCBV)+MRS (LL piki) geleneksel MRG'nin özgüllük oranlarını arttırdığı gözlendi. Relatif serebral kan volümü (rCBV) değeri ve LL piki düşük evre/yüksek evre beyin tümörlerinin farklılaşması için anlamlı olduğu bulunmuştur.
Sonuç: Konvansiyonel MRG'nin preoperatif glioma evrelemesi için yüksek duyarlılığı ve düşük özgüllüğü vardır. MRP ve MRS eklendiğinde konvansiyonel MRG bulgularının özgüllüğü artar.

Anahtar Kelimeler: *Glial hücreli tümörler, perfüzyon manyetik rezonans görüntüleme, manyetik rezonans spektroskopisi*

Geliş tarihi/Received: 12.11.2020
Kabul tarihi/Accepted: 23.11.2020

İletişim:
Turkan Ikizceli, University of Health Sciences, Haseki Training and research Hospital, Department of Radiology, Istanbul, TURKEY.
e-mail: turkan.ikizceli@sbu.edu.tr
Tel: +90 532 455 63 02

JAMER 2020;5(3):25-34

INTRODUCTION

Brain tumors are tumors with the lowest survival rates among malignant tumors (1). The definition of the stage and spread of tumors is significant for the selection of appropriate treatment. As a result, accurate staging before surgery significantly affects survival rates. The role of radiological imaging in early diagnosis and accurate staging has begun to change (2). The first chosen imaging method of Magnetic Resonance Imaging (MRI) has increased sensitivity and specificity with the use of intravenous contrast material, while tumors may have a similar appearance to inflammation, infection, and infarcts (3). Additionally, for assessment of the infiltration of non-contrast tumors, MRI may be insufficient in the differentiation of postoperative residual tumor from postoperative changes or necrosis linked to radiotherapy (4-6). The development of advanced MRI techniques has ensured the possibility of defining the stage and spread of the tumor and planning treatment better (7).

Currently, the advanced MRI techniques that have begun to be used for identification of stage and distribution of cranial tumors include magnetic resonance spectroscopy (MRS) providing information about tissue biochemistry and metabolism, magnetic resonance perfusion (MRP) providing information about tissue microperfusion and diffusion-weighted imaging (DWI) related to microscopic water movements (7,8). MRP is a non-invasive diagnostic method providing information about tissue perfusion at the microscopic level, in-vivo tumor angiogenesis and tumor microcirculation. With this method, information about blood volume, blood flow and tissue oxygen levels are obtained, which cannot be found using conventional MRI (3). The "Epi T2*" sequence is a dynamic imaging method obtained by administering a rapid bolus of contrast material. As paramagnetic contrast material can be administered rapidly, the reduction of T2* effect in brain vascular structures and signal loss in white matter can be imaged (first-pass perfusion). This signal loss is used to calculate time/intensity curves for each voxel and cerebral blood volume (CBV), relative cerebral blood flow (rCBF), mean transit time (MTT) and time to peak (TTP) maps are obtained. The most valuable parameter is the relative cerebral blood volume (rCBV) ratio obtained from CBV (8). On MRP, it is well-known that high-stage tumors show relatively high cerebral blood flow (CBF) values compared to low-stage tumors (9). The CBV values measured in the peritumoral area can be used to differentiate between metastasis-linked edema or high-stage tumors (9,10).

Similarly, recurrent tumor-radiation necrosis differentiation can be performed with perfusion measurements (11). MRS is a non-invasive technique ensuring in-vivo analysis of metabolites in particular tissue to identify the biochemical structure of the underlying pathologies. Metabolites containing protons in tissues are measured with suppression of water and fat signals (12).

Our aim in this study was to obtain information about the tumor stage and distribution and to reveal their contribution to diagnosis by adding MRP and MRS to the conventional MRI sequences of cases considered to have a cerebral glial tumor as a result of MRI investigation.

MATERIAL AND METHODS

Patient Selection: This study was prospectively completed from April 2010 to March 2011 in the radiology department of a university hospital. Consent was obtained from the Ethics Committee of Erciyes University (Date:05.08.2010, Decision number:2010/79) and adhered to the Human Rights Declaration of Helsinki throughout the study.

MRI investigation identified 58 patients with primary glial tumors with a single lesion and supratentorial and intra-axial localization. Of these patients, 26 (12 female, 14 males, mean age 45.6±17.3 years, age interval: 18-73 years) with histopathologic diagnosis of the glial tumor were included in the study. Patients with emergency herniation, taken for emergency surgery, who could not tolerate MRP and MRS tests, with metastasis after pathology and without surgical procedures performed, were excluded from the study.

MRI Imaging: The study used a 1.5 T MR device (Philips Medical Systems, Best, The Netherlands), with all cases lying in the supine position with heads in a standard head coil. Parameters for conventional MRI with T1 SE axial images were slice thickness 5 mm, gap 1 mm, TE 15, TR 623, FOV 137-320, FA 69, matrix 256x256. For T2 TSE axial images, slice thickness was 5 mm, gap 1 mm, TE 110, TR 5068, FOV 137-250, FA 90 and matrix 256x256. For FLAIR axial images, slice thickness was 5 mm, gap 1 mm, TE 120, TR 6000, TI 2000, FOV 137-300, FA 90 and matrix 256x256. For T2 TSE coronal images, slice thickness was 6 mm, gap 1 mm, TE 110, TR 4000, FOV 125-250, FA 90 and matrix 256x256. For T1 SE sagittal images, slice thickness was 5 mm, gap 1 mm, TE 15, TR 488, FOV 107-340, FA 69 and matrix 256x256. Conventional MRI, MRP and MRS images were taken sequentially in a single session. Before the procedure, an 18-20-gauge catheter was inserted in the antecubital vein. The duration of the process was determined as nearly 40 minutes.

Pre-contrast images included T1-Weighted images in axial and sagittal planes, T2-weighted images in the axial and co-

ronal plane and FLAIR images in the axial plane. Contrast images were taken after the MRP investigation.
Conventional MRI investigations assessed findings related to contrast involvement in lesions, presence of necrosis, findings of peritumoral vasogenic edema and mass effect, and presence of internal hemorrhage in the mass.

For staging using conventional MRI, high-stage glioma was differentiated from low-stage glioma by having necrosis/cyst and hemorrhage areas within the tumor, clear edema and mass effect surrounding the tumor and intense contrast involvement in the tumoral area.

MRP Imaging: During imaging, the "Med-Rad Spectris" automatic MRI injection system was used to administer bolus injection of gadopentetic acid dimeglumine (Magnevist-Schering, AG, Germany) contrast agent as 5 ml/s speed with 0.3 mmol/kg dose during a few sections and MRP was begun.

Dynamic susceptibility contrast MRI investigation was performed to obtain perfusion images. 3D scan mode, fast field echo (FFE) technique was used with the EPI rapid imaging method to investigate perfusion. The imaging parameters were TR 17, TE 25, flip angle 7, EPI factor 17, FOV 200, slice thickness 3.5 mm, slice interval 0, NEX 1.0, matrix 128x64, acquisition time 1 min 17 s, and slice number 30.

Perfusion MR imaging duration was a total of 1 minute 17 seconds, with a total of 1200 raw images obtained with a gradient-echo echoplanar imaging sequence. These raw images were sent to a Philips View forum computer workstation for the processing of perfusion data, and rCBV, CBF and MTT maps and quantitative values related to the region were obtained.

The region of interest (ROI) was placed in tissue distant from vascular structures, distant from necrotic and cystic areas, at the boundary of the tumor, and in tissue with normal appearance around the contrast tumors with abnormal MR signals and around contrast tumors or non-contrast tumors. According to the lesion size, ROIs of 30 mm^2 dimensions were used. Three to five ROI were placed in lesions, and the highest rCBV values were selected. The highest ROI as compared with white matter from the opposite hemisphere.
rCBV ratio = max rCBV (tumor)/rCBV (normal)

MRS Imaging: After obtaining MRP images, the identified lesions were assessed with two-dimensional (2D) multivoxel MRS. The spectroscopic investigation was performed after IV contrast material was administered. In selecting the region for investigation, the T2-Weighted axial and contrast T1-Weighted images were used. MRS investigations used the PRESS technique with 1500/144 (TR/TE) values. The device automatically selected water suppression and shimming settings. In the axial or coronal plane, mean 2-8 cm^3 voxel dimensions based on lesion size were chosen inappropriate slices. The voxel was placed to contain the gross pathology, generally the solid or necrotic section of the tumoral region. The procedure took nearly 20 minutes. When determining the area to be investigated, to avoid the negative effect of fat in the subcutaneous area and diploe distance, attempts were made to stay away from calvarial bone structures and also away from CSF and sinus cavities due to negative effects on the spectrum.

The metabolite resonance localizations were determined as follows Cho 3.22 ppm; Cr 3.02 ppm; NAA 2.02 ppm; lipid 0.50-1.50 ppm; lactate 1.33 ppm with TE 144.00msn defining a typical double inverse peak. Maximum Cho/Cr and Cho/NAA ratios were calculated. The presence of lactate and lipid peaks was researched.

Statistical analysis
The analysis of the data was done on the computer using the SPSS 15.0 (IBM Corp., Armonk, NY, USA) statistical software. Normal distribution of data was examined with the Shapiro-Wilks test. A comparison of two groups with a normal distribution of variables used the student t-test, with the Mann-Whitney U test used for variables with non-normal distribution. The chi-square test exact method was used to compare two qualitative variables. The sensitivity and specificity values for differentiation of low- and high-stage tumors were calculated. ROC analysis was performed for the differentiation of two groups using rCBV values. All statistical analyses accepted $p<0.05$ as significant.

RESULTS

Of the 26 cases included in the study, 7 (27%) had low-stage (stage II), and 19 (73%) had high-stage (stage III and IV) CNS tumors. The mean age in the low-stage group was 30.28±8.63 years, while the mean age in the high-stage group was 51.31±16.30 years. There was a statistically significant difference found in terms of age for low-stage/high-stage differentiation ($p<0.05$).

Conventional MRI Findings: The parameters assessed with conventional MRI investigations identified 3 (43%) of the seven low-stage tumors as high-stage tumors. Of the 19 high-stage tumors, 19 (100%) were radiologically identified as high-stage tumors. For low/high stage tumor differentiation, the sensitivity of conventional MRI staging was 100%, with

a specificity of 57%. After administering IV contrast material, contrast involvement was observed in 29% of low-stage tumors and all high-stage tumors (100%) (p<0.05).

Mass effect was observed in 14% of low-stage tumors and 84% of high-stage tumors (p<0.05). Edema was observed in 14% of low-stage tumors and all high-stage tumors (100%) (p<0.05). In terms of hemorrhage findings, there was no statistically significant difference identified for low-stage/high-stage differentiation (p>0.05). Necrosis was observed in 14% of low-stage tumors and 90% of high-stage tumors (p<0.05) (Table 1). Mass effect had 84% sensitivity and 86% specificity. For edema, necrosis, and contrast involvement, the sensitivities were 100%, 90%, and 100%, with specificities of 86%, 86%, and 71%, respectively (Table 2).

Table 1. Efficacy of conventional MRI findings for high-/low-stage differentiation of glial tumors

		Low-stage n (%)	High-stage n (%)	χ^2	p
Mass Effect	Yes (17)	1 (%14)	16 (%84)	11.051	**0.02 (<0.05)**
	No (9)	6 (%86)	3 (%16)		
Edema	Yes (20)	1 (%14)	19 (%100)	21.171	**0,000 (<0.05)**
	No (6)	6 (%86)	0 (%0)		
Hemorrhage	Yes (4)	1 (%14)	3 (%16)	0.009	**1,000 (>0.05)**
	No (22)	6 (%86)	16 (%84)		
Necrosis	Yes (18)	1 (%14)	17 (%90)	13.576	**0,001 (<0.05)**
	No (8)	6 (%86)	2 (%11)		
Contrast Enhancement	Yes (21)	2 (%29)	19 (%100)	16.803	**0,000 (<0.05)**
	No (5)	5 (%71)	0 (%0)		

Table 2. Sensitivity and specificity percentages of MRI for low-stage/high-stage differentiation of tumors

	Sensitivity (%)	Specificity (%)
Mass Effect	84	86
Edema	100	86
Hemorrhage	16	86
Necrosis	90	86
Contrast Enhancement	100	71

MRP Findings: Low-stage tumors had rCBV values of 0.90-2.16, rCBF values 0.52-4.08 and MTT values of 0.36-2.29, while high-stage tumors had rCBV values 0.99-7.50, rCBF values 0.56-8.33 and MTT values 0.31-3.60 (Table 3) (Figure 1a,b,c).

In our study, rCBV value was found to be significant for differentiation of low-stage/high-stage brain tumors (p<0.05), while rCBF and MTT values were not significant for differentiation of low-stage/high-stage tumors (p>0.05) (Table 4).

ROC analysis of rCBV values for differentiation of low-stage/high-stage tumors found the threshold value for rCBV was 2.16. For this value, sensitivity was 58%, while specificity was 100% (Figure 2).

MRS Findings: For low-stage tumors, the Cho/Cr ratios were 1.59 to 2.47, and Cho/NAA ratios were 0.37 to 4.94, while high-stage tumors had Cho/Cr ratios 0.87 to 4.89 and Cho/NAA ratios 0.24 to 10.20 (Table 5) (Figure 3a-d).

For low-stage/high-stage differentiation, Cho/Cr ratios and Cho/NAA ratios were not found to be significant (p>0.05). The LL peak was 29% for low-stage tumors and 90% for high-stage tumors (p<0.05). The LL peak had a sensitivity of 90% and specificity of 71% for differentiation of low-stage/high-stage tumors. After separately assessing the sensitivity and specificity rates for conventional MRI, MRP, and MRS, the combined use of conventional MRI+MRP (rCBV), conventional MRI+MRS (LL peak) and conventional MRI+MRP (rCBV)+MRS (LL peak) were observed to increase the specificity rates of conventional MRI (Table 6) (Figure 4a-d).

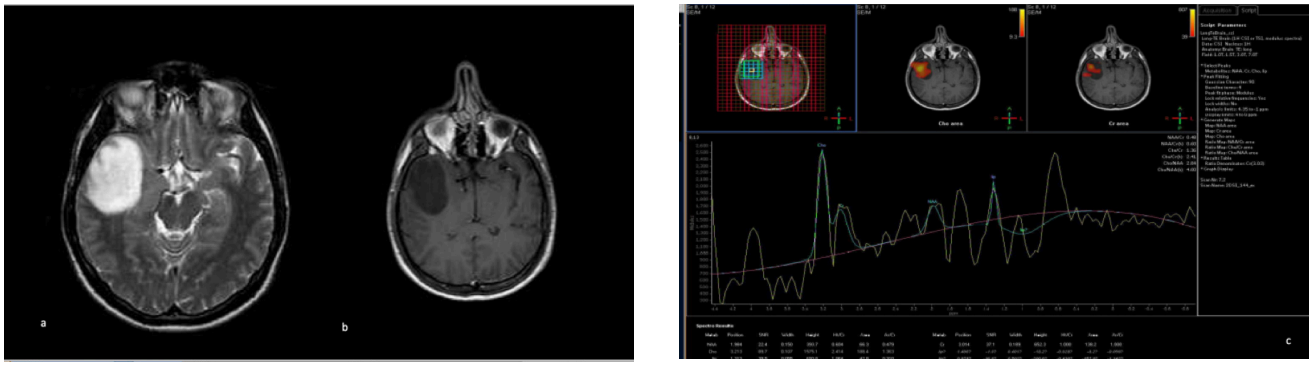

Figure 1. 25-year-old male patient (patient no:5) a) T2 weighted image shows a hyperintense mass lesion in the right temporal region. b) T1weighted contrast image does not show significant contrast enhancement in the lesion. c) In the rCBV map, there is no significant increase in blood flow in the lesion (rCBV: 1.12).

Table 3. MR perfusion rCBV, rCBF and MTT values for low (patient no: 1-7) and high-stage (patient no: 8-26) tumors

Patient	Age	Sex	rCBV	rCBF	MTT	Pathology
1	44	M	0.90	0.52	1.73	Fibrillary Astrocytoma, Stage II
2	37	F	2.09	3.15	0.66	Oligoastrocytoma, Stage II
3	25	M	2.08	4.08	0.55	Fibrillary Astrocytoma, Stage II
4	33	M	2.10	1.42	1.47	Astrocytoma, Stage II
5	25	M	1.12	1.01	1.10	Astrocytoma, Stage II
6	30	F	2.16	0.94	2.29	Oligodentroglioma, Stage II
7	18	M	1.13	3.13	0.36	Epandimoma, Stage II
8	73	F	5.40	8.33	0.64	Glioblastoma, Stage IV
9	45	F	2.86	1.84	1.55	Anaplastic Astrocytoma, Stage III
10	45	F	7.50	5.71	1.31	Primitive Neuroectodermal Tumor, Stage IV
11	66	F	3.72	3.97	0.93	Glioblastoma, Stage IV
12	64	M	2.06	0.80	2.57	Glioblastoma, Stage IV
13	72	M	3.28	4.19	0.78	Glioblastoma, Stage IV
14	18	F	4.07	4.67	0.87	Anaplastic Astrocytoma, Stage III
15	53	M	3.81	3.39	1.12	Glioblastoma, Stage IV
16	44	M	4.54	2.85	1.59	Glioblastoma, Stage IV
17	19	M	2.09	2.30	0.90	Primitive Neuroectodermal Tumor, Stage IV
18	35	F	1.68	2.76	0.60	Glioblastoma, Stage IV
19	66	F	1.92	1.88	1.02	Glioblastoma, Stage IV
20	56	M	2.02	0.56	3.60	Glioblastoma, Stage IV
21	45	F	3.94	2.50	1.57	Recurrence, Glioblastoma, Stage IV
22	61	M	4.83	2.38	2.02	Glioblastoma, Stage IV
23	41	F	3.93	2.78	1.41	Recurrence, Germiocytic Astrocytoma, Stage III
24	50	F	1.15	3.70	0.31	Glioblastoma, Stage IV
25	49	M	0.99	0.99	1.00	Glioblastoma, Stage IV
26	73	M	2.07	1.48	1.39	Glioblastoma, Stage IV

Table 4. rCBV, rCBF and MTT values according to groups

	rCBV (mean±SD)	p	rCBF (mean±SD)	MTT (mean±SD)	p
Low Stage	1.65±0.57	(<0.05)	2.03±1.38	1.16±0.70	p>0.05
High Stage	3.25±1.64		3.00±1.86	1.32±0.76	p>0.05

rCBV: Relative Cerebral Blood Volume, **rCBF**: Relative Cerebral Blood Flow, **MTT**: Mean Transit Time, **SD**: Standard Deviation

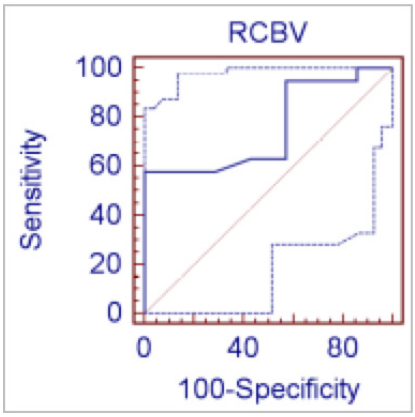

Figure 2. ROC curve for rCBV

Table 5. MRS findings for low (patient no: 1-7) and high-stage (patient no: 8-26) tumors

Patient	Age	Sex	Cho/NAA	Cho/Cr	LL+/-	Pathology
1	44	M	1,42	2,15	(-)	Fibrillary Astrocytoma, Stage II
2	37	F	0,37	2,28	(-)	Oligoastrocytoma, Stage II
3	25	M	1,76	2,47	(-)	Fibrillary Astrocytoma, Stage II
4	33	M	1,34	1,59	(-)	Astrocytoma, Stage II
5	25	M	4,00	2,41	(+)	Astrocytoma, Stage II
6	30	F	4,94	2,32	(+)	Oligodentroglioma, Stage II
7	18	M	1,84	1,87	(-)	Epandimoma, Stage II
8	73	F	0 ,69	3,02	(+)	Glioblastoma, Stage IV
9	45	F	0 ,24	3,65	(+)	Anaplastic Astrocytoma, Stage III
10	45	F	3,82	2,76	(+)	Primitive Neuroectodermal Tumor, Stage IV
11	66	F	4,28	3,66	(+)	Glioblastoma, Stage IV
12	64	M	0,55	2,57	(+)	Glioblastoma, Stage IV
13	72	M	1,51	2,17	(+)	Glioblastoma, Stage IV
14	18	F	0,81	3,23	(+)	Anaplastic Astrocytoma, Stage III
15	53	M	2,83	2,96	(+)	Glioblastoma, Stage IV
16	44	M	0,40	3,10	(+)	Glioblastoma, Stage IV
17	19	M	6,51	4,89	(+)	Primitive Neuroectodermal Tumor, Stage IV
18	35	F	10,20	1,77	(-)	Glioblastoma, Stage IV
19	66	F	4,26	2,58	(+)	Glioblastoma, Stage IV
20	56	M	1,34	1,79	(+)	Glioblastoma, Stage IV
21	45	F	2,75	1,66	(+)	Recurrence, Glioblastoma, Stage IV
22	61	M	0,36	0, 87	(+)	Glioblastoma, Stage IV
23	41	F	4,19	3,73	(+)	Recurrence, Germiocytic Astrocytoma, Stage III
24	50	F	0,92	1,08	(+)	Glioblastoma, Stage IV
25	49	M	2,11	3,56	(-)	Glioblastoma, Stage IV
26	73	M	1,41	1,97	(+)	Glioblastoma, Stage IV

M: Male, **F:** Female, **Cho:** Choline, **NAA:** N-Acetyl Aspartate, **Cr:** Creatine, LL: Lipid Lactate.

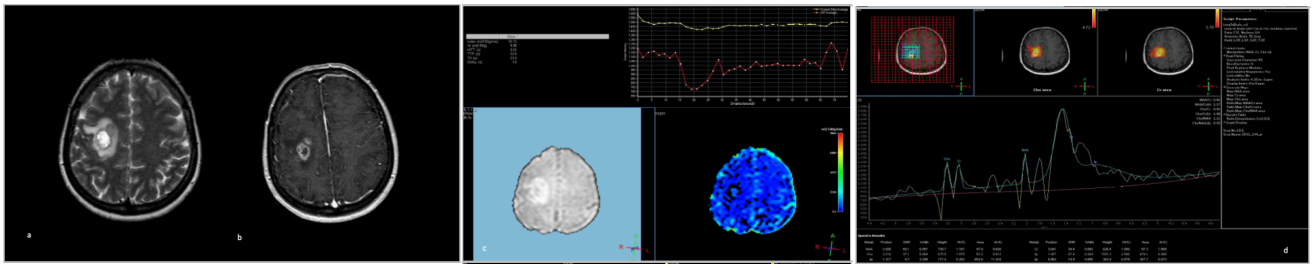

Figure 3. 50-year-old female patient (patient no:24) a,b) T2 weighted image shows a mass lesion in the right frontal region that has a cystic feature and an anterior wall component and vasogenic edema around it. c) There was no increase in perfusion in rCBV map (rCBV: 1.15). d) In the contrast-enhanced area of MRS (Histopathological diagnosis: GBM, stage IV)

Table 6. Sensitivity and specificity for conventional MRI, MRP, MRS, conventional MRI+MRP (rCBV), conventional MRI+MRS (LL peak) and conventional MRI+MPR (rCBV)+MRS (LL peak) for differentiation of low-stage/high-stage tumors

	Sensitivity (%)	Specificity (%)
MRI	100	57
MRP (rCBV)	58	100
MRS (LL piki)	90	71
MRI+MRP (rCBV)	100	100
MRI+MRS (LL)	100	71
MRI+MRP (rCBV)+MRS (LL)	100	100

MRI: Magnetic Resonance Imaging, **MRP:** Perfusion Magnetic Imaging, **MRS:** Magnetic Resonance Spectroscopy, **LL:** Lipid Lactate, **rCBV:** Relative Cerebral Blood Volume

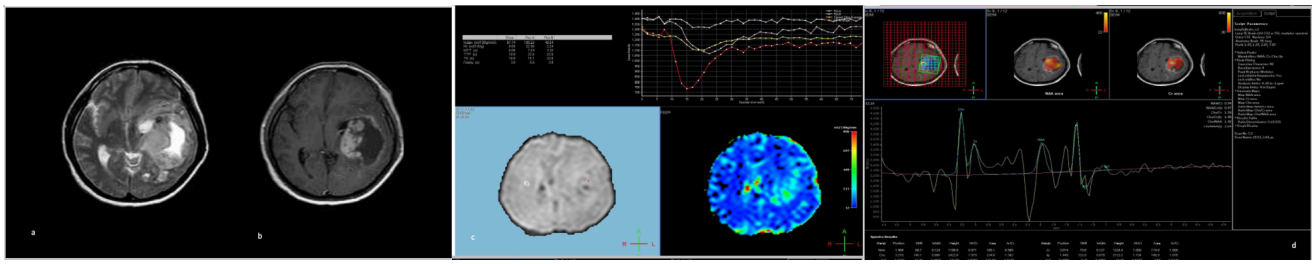

Figure 4. A 45-year-old female patient (patient no:10) a,b) T2 weighted and contrast-enhancement image, a mass lesion with the heterogeneous hyperintense feature in the left temporal region and vasogenic edema around it. c) The rCBV map shows a marked perfusion increase in the lesion (rCBV: 7.50). d) In the contrast-enhanced regions of MRS, the presence of LL peak is observed, Pathology: Primitive Neuroectodermal Tumor (PNET) stage IV.

DISCUSSION

The glioma staging accuracy rate for conventional MRI varies from 55-83% in studies (13). High-stage glioma is differentiated from low-stage glioma due to intense contrast involvement, peritumoral edema, necrosis/cyst, and hemorrhage areas within the tumor and showing mass effects (14). Staging frequently uses samples taken from parts of the tumor with contrast. There is a rough link between contrasting and tumor stage (2). Of high-stage tumors with contrast expected, 40% do not have contrast involvement, while some low-stage tumors may involve contrast and even have peritumoral edema leading to mistaken assessment as high-stage tumors (15-17). Peritumoral edema is a good marker for high-stage tumors. However, some studies have identified that the peritumoral areas may be malig-

nant. The tumor is not limited to the areas with contrast involvement but may extend into the edema area (18). As a result, the appearance of vasogenic edema areas may be a combination of intracerebral edema and infiltrative tumor (19-21). In our study, MRI staging had a 100% accuracy rate for high-stage tumors, with contrasting and peritumoral edema in all 19 high-stage tumors. There was no high-stage tumor without contrast involvement in our study. Of the seven low-stage tumors, two had contrasting, one case had an intratumoral hemorrhage, one case had necrosis, and one case had the mass effect, which lowered the sensitivity (57%). In the literature, intratumoral hemorrhage is emphasized as a trait of high-stage tumors but is said to be present in some low-stage tumors (2). In our study, the low number of cases and unequal numbers in the two groups may have caused this result.

Increasing vascularity in brain tumors may be measured concretely with rCBV (2). High-stage tumors show higher vascularity (18). Studies have shown that rCBV values may be beneficial for preoperative glioma staging. In the literature, there are very different results related to rCBV values, with the threshold value of 1.5 used by Lev et al. for non-contrast high-stage tumors having 100% sensitivity and 69% specificity (6). Law et al. concluded the rCBV and rCBF measurements were well-correlated with histopathologic staging, while MTT was not useful to distinguish glioma stage (4). Zonari et al. reported rCBV was the most valuable parameter. In our study, we found a threshold value of 2.16, and the rCBV of low-stage tumors was 1.65±0.57 and 3.25±1.64 for high-stage tumors ($p<0.05$). The sensitivity of this threshold value was 58%, with a specificity of 100%. The rCBF and MTT values were not found to be significant for low-stage/high-stage differentiation ($p>0.05$). There are very limited studies where rCBF was found to be significant. As most cases included in the study had high-stage tumors, the rCBV values were found to be high. However, though 8 cases had a high-stage tumor, they were below the rCBV threshold value, which lowered the sensitivity. In the literature, the reason technical sensitivity of MRP investigation is significant is due to situations like blood products disrupting homogeneity of the magnetic area, presence of calcium, melanin and metals, difficulties accurately assessing lesions with localization close to brain-bone and bone-air interfaces and intravenous contrast leak in pathologies that severely disrupt the blood-brain barrier (GBM, etc.) causing erroneous assessment (15). Variations in heart functions and variations in vascular or collateral circulation may make it difficult to interpret perfusion maps, with major arterial occlusion causing the widening of the time-concentration curve due to collateral circulation. In these situations, it is reported that parameters will be calculated below their true values (22).

The most important parameters for histologic assessment of tumor stage are mitotic activity, necrosis, and vascular proliferation (23). Glial tumors generally have high Cho/Cr ratios; however, there is glial neoplasia reported without elevated Cho/Cr ratios. The results of much research, surprisingly, show that the Cr levels are the same in both low and high-stage glioma. Additionally, previous studies have shown that low Cr levels may be observed in brain tumors. Additionally, the Cr amount may show variations in different regions of the same tumor. Hypometabolic areas of the same tumor may have high Cr, while hypermetabolic areas may show reduced Cr (23). Kinoshita et al. showed that high-stage tumors have higher Cho, lower NAA and Cr ratios compared to low-stage tumors (24). One cause of the variable results is that gliomas have heterogeneous histologic and metabolic structure. Additionally, the Cho value shows tumor cellularity, and tumor cellularity may not directly reflect tumor stage (23). A broad-series study of 120 cases compared high-stage and low-stage tumors and concluded that the combination of Cho/NAA, Cho/CR ratios, and LL peaks was reliable for the staging of glioma (25). Studies have shown that the presence of lactate peak in low-stage tumors may indicate malignant transformation (24), reporting that the lactate peak may be observed after RT and after the operation (26). Additionally, as lactate may be identified in all cystic areas, it should not be forgotten that lactate peaks may be observed in some low-stage neoplasms containing cystic areas. MRS investigation identifying lipid peak in solid tumoral lesions caused the consideration that these tumors should be accepted as malignant until proven otherwise (27,28). In our study, Cho/Cr and Cho/NAA ratios were similarly not found to be significant for low-stage/high-stage differentiation ($p>0.05$). The LL peak had 90% sensitivity and 71% specificity for differentiation of low/high stage glial tumors. Most of the cases included in the study had high-stage tumors, containing intense necrotic areas with reduced Cho/Cr ratios in necrotic lesions and contrary to this, we believe increased LL peak. The observation of LL peaks in 2 of the seven low-stage tumors leads us to think that this may be linked to cystic contents in low-stage tumors. Additionally, the two tumor groups may not be homogeneous and contain different histopathologic tumor types. Though in the same stage, tumors with different histopathology, different appearance and different values may have affected statistical parameters.

Studies adding MRP and MRS to conventional sequences have different results in terms of superiority for tumor sta-

ging. Fayed et al. stated MRS was better than MRP (29). Spampinato et al., contrarily, stated MRP was more valuable than MRS (30). Costanzo et al. found the combination of LL peak and rCBV values had 100% accuracy for tumors and 90% accuracy for tumor boundaries (31). Chawla et al. identified that MRS and MRP were complementary to each other (32). In our study, conventional MRI had 100% sensitivity and 57% specificity for tumor stage differentiation, while sensitivity was 100% and specificity was 100% when used with MRP. When conventional MRI and MRS are used together, sensitivity was 100%, with the specificity of 71%. When MRP and MRS are used with conventional MRI, specificity increased (100%). The MRP parameter of rCBV and the MRS parameter of the LL peak was found to be valuable, with the use of these two parameters with conventional MRI shown to be complementary. The addition of MRP and MRS to conventional sequences lengthens the procedure duration and lowers patient tolerance, which led to low case numbers, an important limitation of our study.

CONCLUSION

Conventional MRI has high sensitivity and low specificity for preoperative glioma staging. The specificity of conventional MRI findings increases when MRP and MRS are added to it. While for conventional sequences, contrasting, perilesional edema, necrosis and mass effect are important, rCBV on MRP and LL peak on MRS are important parameters.

Acknowledgment: Authors thank Dr. Halil Dönmez, Dr. İ Suat Oktem and Dr. Ferhan Elmalı.

Conflict of Interest: No conflict of interest was declared by the authors.

Financial Disclosure: The authors declared that this study has received no financial support.

Ethics Committee Approval: The study was approved by the Ethics committee of Erciyes University.

Informed Consent: Informed consent were taken all patients that included the study.

Author Contributions: Conception/Design of Study- S.K.; Data Acquisition- S.K., T.İ; Drafting Manuscript- T.İ; Critical Revision of Manuscript- S.K., T.İ; Final Approval and Accountability- S.K., T.İ; Supervision- T.İ.

REFERENCES

1. Shukla G, Alexander GS, Bakas S, Nikam R, Talekar K, Palmer JD, et al. Advanced magnetic resonance imaging in glioblastoma: a review. Chin Clin Oncol. 2017;6(4):40.

2. Covarrubias DJ, Rosen BR, Lev MH. Dynamic magnetic resonance perfusion imaging of brain tumors. The Oncologist. 2004;9:528-37.

3. Metaweh NAK, Azab AO, El Basmy AAH, Mashhour KN, El Mahdy WM. Contrast-Enhanced Perfusion MR Imaging to differentiate between recurrent/residual brain neoplasms and radiation necrosis. Asian Pac J Cancer Prev. 2018;19(4):941-48.

4. Law M, Yang S, Wang H, Babb JS, Johnson G, Cha S, et al. Glioma grading: sensitivity, specificity, and predictive values of perfusion MR imaging and proton MR spectroscopic imaging compared with conventional MR imaging. AJNR. 2003;24:1989-98.

5. Aksoy FG, Lev MH. Dynamic contrast-enhanced brain perfusion imaging: Technique and clinical applications. Semin Ultrasound CT MRI. 2000;21:462-77.

6. Lev M, Rosen B. Clinical applications of intracranial perfusion MR imaging. Neuroimaging Clin North Am. 1999;9:309-31.

7. Yang D, Korogi Y, Sugahara T, Kitajima M, Shigematsu Y, Liang L, et al. Cerebral gliomas: prospective comparison of multivoxel 2D chemical-shift imaging proton MR spectroscopy, echoplanar perfusion and diffusion-weighted MRI. Neuroradiology. 2002;44:656-66.

8. Aksoy FG, Yerli H. Dinamik kontrastlı beyin perfüzyon görüntüleme: teknik prensipler, tuzak ve sorunlar. Tanısal ve Girişimsel Radyoloji. 2003;9:309-14.

9. Calli C, Kitis O, Yunten N, Yurtseven T, Islekel S, Akalin T. Perfusion and diffusion MR imaging in enhancing malignant cerebral tumors. Eur J Radiol 2006;58:394-403.

10. Gupta PK, Saini J, Sahoo P, Patir R, Ahlawat S, Beniwal M, et al. Role of Dynamic Contrast-Enhanced Perfusion Magnetic Resonance Imaging in grading of pediatric brain tumors on 3T. Pediatr Neurosurg. 2017;52(5):298-305.

11. Rollin N, Guyatat J, Streichenberger N, Honnorat J, Tran Minh VA, Cotton F. Clinical relevance of diffusion and perfusion magnetic resonance imaging in assessing intra-axial brain tumors. Neuroradiology. 2006;48:150-9.

12. Warren KE. NMR spectroscopy and pediatric brain tumors. Oncologist. 2004;9:312-8.

13. Zonari P, Baraldi P, Crisi G. Multimodal MRI in the characterization of glial neoplasms: the combined role of single-voxel MR spectroscopy, diffusion imaging and echo-planar perfusion imaging. Neuroradiology. 2007;49:795-803.

14. Wilms G, Demaerel P, Sunaert S. Intra-axial brain tumours. Eur Radiol. 2005;15:468-84.

15. Batra A, Tripathi RP, Singh AK. Perfusion magnetic resonance imaging and magnetic resonance spectroscopy of cerebral gliomas showing imperceptible contrast enhancement on conventional magnetic resonance imaging. Australas Radiol. 2004;48:324-32.

16. Lee SJ, Kim JH, Kim YM, Wog K. Perfusion MR imaging in gliomas: comparison with histologic tumour grade. Korean J Radiol. 2001;2:1-7.

17. Calli C, Kitis O, Yunten N, Yurtseven T, Islekel S, Akalin T. Perfusion and diffusion MR imaging in enhancing malignant cerebral tumors. Eur J Radiol. 2006;58:394-403.

18. Knopp E, Cha S, Johnson G, Mazumdar A, Golfinos JG, Zagzag D, et al. Glial neoplasms: dynamic contrast-enhanced T2*-weighted MR imaging. Radiology. 1999;211:791-8.

19. Pronin IN, Holodny AI, Petraikin AV. MRI of high-grade glial tumors: correlation between the degree of contrast enhancement and the volume of surrounding edema. Neuroradiology. 1997;39:348-50.

20. Holt RM, Maravilla KR. Supratentorial gliomas: Imaging. In: Wilkins RH, Rengachary SS. (eds.) Neurosurgery. McGraw-Hill, New York, 1996;753-88.

21. Kelly WM, Brant-Zawadzki B. Magnetic resonance imaging and computed tomography of supratentorial tumors. Radiology. 1990;3:1-22.

22. Soonmee C, Edmond A.K, Johnson G, Wetzel SG, Litt AW, Zagzag D. Intracranial mass lesions: Dynamic contrast-enhanced susceptibility-weighted echoplanar perfusion MR imaging. Radiology. 2002;223:11-29.

23. Yerli H, Agildere AM, Ozen O, Geyik E, Atalay B, Elhan AH. Evaluation of cerebral glioma grade by using normal side creatine as an internal reference in multi-voxel 1H-MR spectroscopy. Diagn Interv Radiol. 2007;13:3-9.

24. Kinoshita Y, Kajiwara H, Yokota A, Koga Y. Proton magnetic resonance spectroscopy of brain tumors: an in vitro study. Neurosurgery. 1994;35:606-13.

25. Segebarth CM, Baleriaux DF, Luyten PR, Den Hollander JA. Detection of metabolic heterogeneity of human intracranial tumors in vivo by 1H NMR spectroscopic imaging. Magn Reson Med. 1990;13:62-76.

26. Warren KE, Frank JA, Black JL, Hill RS, Duyn JH, Aikin AA, et al. Proton magnetic resonance spectroscopic imaging in children with recurrent primary brain tumors. J Clin Oncol. 2000;18:1020-6.
27. Usenius JP, Kauppinen RA, Vainio PA, Hernesniemi JA, Vapalahti MP, Paljärvi LA, et al. Quantitative metabolite patterns of human brain tumors: detection by 1H NMR spectroscopy in vivo and in vitro. J Comput Assist Tomogr. 1994;18:705-13.
28. Usenius JP, Vainio P, Hernesniemi J, Kauppinen RA. Choline-containing compounds in human astrocytomas studied by 1H NMR spectroscopy in vivo and in vitro. J Neurochem. 1994;63:1538-43.
29. Fayed N, Modrego PJ. The contribution of magnetic resonance spectroscopy and echoplanar perfusion-weighted MRI in the initial assessment of brain tumors. J Neurooncol. 2005;72:261-5.
30. Spampinato MW, Smith JK, Kwock L, Ewend M, Grimme JD, Camacho DL, et al. Cerebral blood volume measurements and proton MR spectroscopy in grading of oligodendroglial tumors. AJR Am J Roentgenol. 2007;188:204-12.
31. Di Costanzo A, Scrabino T, Trojsi F, Giannatempo GM, Popolizio T, Catapano D, et al. Multiparametric 3T MR approach to the assessment of cerebral gliomas: tumor extent and malignancy. Neuroradiology. 2006; 48:622-31.
32. Chawla S, Wang S, Wolf RL, Woo JH, Wang J, O'Rourke DM, et al. Arterial spin-labeling and MR spectroscopy in the differentiation of gliomas. Am J Neuroradiol. 2007; 28:1683-9.